

Controlling interlayer spacing of GO membranes via the insertion of GN for high separation performance

Xuan Liu^{*1}, Zhu Zhou¹, Hengzhang Dai¹, Kuang Ma¹, Yafei Zhang^{2a} and Bin Li^{**3}

¹College of Engineering, Shanghai Ocean University, 999 Huchenghuan Road, Pudong New Area District Shanghai, P.R.China

²Ministry of Education Key Laboratory for Thin Membrane and Microfabrication Technology, Research Institute of Micro/Nanometer Science and Technology, Shanghai Jiao Tong University, 800 Dongchuan Road, Minxing District, Shanghai, P.R.China

³Research Center for Photovoltaics, Shanghai Institute of Space Power-Sources, 2952 Dongchuan Road, Minhang District, Shanghai, 200245, China

(Received December 23, 2020, Revised June 27, 2023, Accepted June 28, 2023)

Abstract. Graphene oxide (GO) membranes have attracted extensive attention in water treatment and related fields. However, GO films are unstable and have low permeability, which have hindered their further development. In this paper, a simple and effective method was used in which GO and single-layer graphene (GN) were mixed, and the layer spacing was effectively controlled by accurately controlling the ratio of GO to GN. GO-GN composite membranes have excellent stability, salt rejection (95.4%), and water flux (26 L m⁻² h⁻¹ bar⁻¹). This unique design structure can be used for precise and effective regulation of the layer spacing in GO, improving the rejection rate, and increasing water flux via the enhancement of low-friction capillary action. The rational development and use of this unique composite membrane provides a reference for the water treatment field.

Keywords: composite membranes; graphene oxide; interlayer spacing; water treatment

1. Introduction

Membrane separation technology is considered to be one of the most significant scientific means of solving the global water crisis (Haan *et al.* 2018). The ideal membrane should provide high flux, high selectivity, and good stability (Qing *et al.* 2018). However, two inherent trade-offs for traditional membrane materials are permeability and selectivity, and these limit the use of these materials (u *et al.* 2015).

Recently, two-dimensional (2D) materials (Sun *et al.* 2020) have been widely used in separation films because of their interlayer structure (Wang *et al.* 2019). As a new type of 2D nanomaterial, graphene oxide (GO) has been commonly researched because of their structural flexibility, mechanical properties, and single atom thickness (Chen *et al.* 2016, Wang *et al.* 2018). The spacing of GO membranes is a key parameter in determining desalination performance (You *et al.* 2016). However, GO is rich in carboxyl, epoxy, and hydroxyl functional groups, and these make the material very hydrophilic (Zhang and Chung 2017, Syama and Mohanan 2019). When the GO membrane is immersed in water, hydration disrupts hydrogen bonds and increases the d-spacing of the original GO membrane via the insertion

of a water monolayer (Zheng *et al.* 2016). To obtain high-performance films, it is necessary to properly adjust the d-spacing.

It has been proven that regulating the layer spacing of GO can effectively improve the performance of a nano-filtration film. According to the literature, the interlayer spacing can be controlled via physical methods (Zhang *et al.* 2019). For example, embedding stacked GO sheets in epoxy (Abraham *et al.* 2017) or regulating external pressure of GO (Wanbin *et al.* 2018) can be used to control the interlayer spacing.

In addition to physical strategies, some chemical strategies have also been proposed for regulating interlayer spacing. Introducing small molecule cross-linking (Yu *et al.* 2017, Thebo *et al.* 2018) and macromolecule or nanomaterial intercalation (Chen *et al.* 2018, Han *et al.* 2015) modify GO membranes. However, there are two problems. On one hand, the inherent geometry of molecules between GO nanosheets makes it difficult for these methods to obtain interlaminar channels that are small enough for desalination (Guoke *et al.* 2019). On the other hand, nanoscale intercalation agents (such as multiwalled carbon nanotubes (Han *et al.* 2015) make it difficult to obtain uniform nanochannels. In addition, the interlayer spacing can also be adjusted by reducing graphene oxide. Reduction methods mainly include heat annealing reduction (Shao *et al.* 2015), microwave irradiation (MWI) reduction (Tang *et al.* 2019), photo-irradiation reduction (Wan *et al.* 2019, Tiwari *et al.* 2020), chemical reagent reduction (Pei *et al.* 2010, Suri *et al.* 2016), photocatalyst reduction (Wei *et al.* 2019), electrochemical reduction, and solvothermal reduction (Toh *et al.* 2014, Singh *et al.* 2011). These reduction

*Corresponding author, Ph.D.,
E-mail: xliu@shou.edu.cn

**Corresponding author, Ph.D.,
E-mail: tolb10@163.com

^a Ph.D., Professor, E-mail: yfzhang @sjtu.edu.cn

methods enhance π - π interactions between sheets by reducing the content of oxygen-containing functional groups in GO membranes (Lyu *et al.* 2018), and thus, the GO layer spacing is effectively decreased. However, there is a risk that an impermeable membrane might be obtained (Wanbin *et al.* 2018), and this makes it difficult to meet the exact requirements in practical applications. Hence, effective measures are necessary to regulate layer spacing and to avoid graphitization.

In this study, different proportions GN and GO were mixed to prepare nanofiltration membranes. Precise regulation of the proportion of GN in the mixed materials enables effective control of the layer spacing and avoids graphitization, thus, membrane rejection and water flux can be improved. The rejection and water flux of the composite membrane changed with the ratio of GO and GN. Specifically, the addition of graphene reduces the layer spacing and increases the film thickness to achieve a high rejection of NaCl and Rhodamine B. Moreover, membrane swelling in wet conditions was inhibited, and this endows the membrane with good stability. At the same time, incorporating GN weakened interactions (hydrogen bonding) between water molecules and oxygen-containing functional groups at oxidized regions of the GO nanosheets.

2. Methods

2.1 Materials

Natural graphite powder and single-layer graphene powder (longitudinal dimension: 0.8 nm) were purchased from Shanghai Li Wu Sheng Limited Company. Hydrochloric acid (HCl), hydrogen peroxide (H₂O₂), potassium permanganate (KMnO₄), concentrated sulfuric acid (H₂SO₄), ethanol (C₂H₅OH), sodium nitrate (NaNO₃), Rhodamine B (RB), and sodium chloride (NaCl) were all analytically pure and purchased from Sinopharm Group Chemical Reagent Limited Company. All of the chemicals were used without further purification.

2.2 Preparation of GO and GO-GN hybrid membrane

Synthesis of GO

GO was prepared by using the modified Hummers method (Shao *et al.* 2020). Graphite powder (4 g) was added to a flask. First, 100 mL of concentrated sulfuric acid was added and stirred continuously at low temperature for 30 min. NaNO₃ (2.0 g) was added followed by another 2 h of stirring. Then, sufficient KMnO₄ was added to the reactant to bring the temperature to 35 °C, and the mixture was continuously stirred for 2 h. Afterward, 180 mL of deionized water was added, the temperature was increased to 95 °C, and this was maintained for 15 min. Then, proper amounts of deionized water and H₂O₂ (30%) were added. Finally, hydrochloric acid and deionized water were used to filter and wash the as-prepared GO several times. Dialyzing GO obtain a neutral aqueous solution and freezing and drying.

Synthesis of GO-GN composite membrane

First, GO powder was dispersed and ultrasonicated in

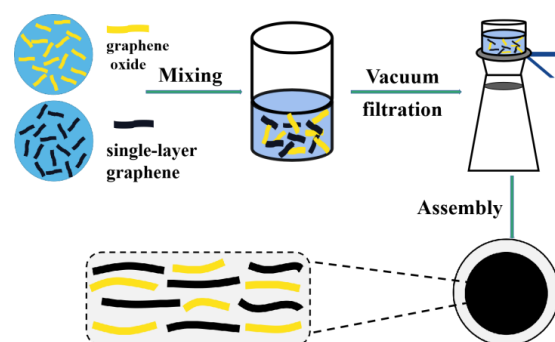


Fig. 1 Preparation process of GO-GN composite membrane

deionized water to obtain 0.1 mg mL⁻¹ GO dispersion. Weighing quality were 0.02 mg, 0.04 mg, 0.06 mg, 0.08 mg, 0.1 mg of the GN, respectively, to join the 5 mL of 0.1 mg mL⁻¹ of GO solution. Then, 40 mL of deionized water was added to each of the five mixtures, and a glass rod was used to fully stir the mixtures. The mixtures were then put into an ultrasonic cleaning machine for ultrasonication so that GO and GN were fully mixed and dispersed in the deionized water. Finally, composite membranes were fabricated on mixed cellulose ester (MCE, 50 mm in diameter, 0.22 μ m in aperture) membranes via vacuum filtration. These membranes were then dried in air (Figs. 1 and S1).

2.3 Characterization

The morphology and microstructure of the GO-GN composite membranes were revealed using scanning electron microscopy (SEM, ZEISS, Gemini SEM7426) and transmission electron microscope (TEM, Thermo Fisher Scientific, Talos L120C G2). Raman spectroscopic characterization was recorded using a Renishaw inVia microscope. The hydrophilicity of the films was investigated using an optical contact angle measuring instrument (Kruss, DSA30), observing the water contact angle of the films. The differences in the d-spacings of the GO-GN membranes were measured via X-ray diffraction (XRD, Bruker, D8 Advance). The amount of Rhodamine B in the organic screening experiment was obtained using an ultraviolet-visible absorption spectrometer (UV-vis, PerkinElmer, LAMBDA950). Furthermore, a miniature sodium ion meter (qiwei instrument co., LTD., Dwa-51) was used to measure the concentrations of ionic solutions in the feed and permeate sides.

2.4 Membrane performance evaluation

The performance of composite membranes was evaluated in terms of water flux, rejection, and stability.

Water flux (*J*)

Water flux were measured on a dead-end filtration system using a vacuum filtration device. The effective area of the films was 3.1 cm², and the applied pressure was 1 bar. The water flux (*J*, L m⁻² h⁻¹ bar⁻¹) of the GO-GN composite membranes was calculated using the following equation:

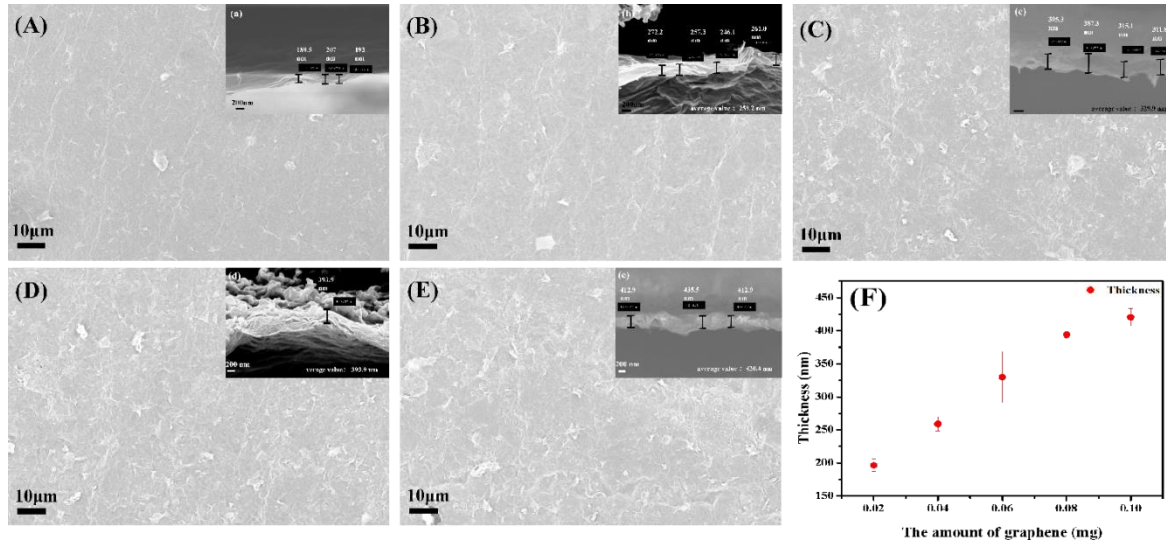


Fig. 2 Surface and cross-sectional SEM images of the GO-GN composite membranes: (A,a) GO_{0.5}-GN_{0.02} (mix of 0.5 mg graphene oxide and 0.02 mg single-layer graphene), (B,b) GO_{0.5}-GN_{0.04} (mix of 0.5 mg graphene oxide and 0.04 mg single-layer graphene), (C,c) GO_{0.5}-GN_{0.06} (mix of 0.5 mg graphene oxide and 0.06 mg single-layer graphene), (D,d) GO_{0.5}-GN_{0.08} (mix of 0.5 mg graphene oxide and 0.08 mg single-layer graphene), (E,e) GO_{0.5}-GN_{0.1} (mix of 0.5 mg graphene oxide and 0.1 mg single-layer graphene). (F) Variations in membranes

$$J = \frac{V}{A \times \Delta t \times P} \quad (1)$$

V is the volume of water that passes through the membrane, A is the effective area of the membrane, Δt is the filtration time, and P is the filtration pressure.

Rejection (R)

The desalination rate (R , %) of the films was measured via free diffusion. To test the GO-GN composite membranes, 80 mL of 1000 ppm NaCl solution and 80 mL of deionized water were added to the feeding side and permeate side, respectively. The rejection R (%) was calculated according to the following equation:

$$R = \left(1 - \frac{C_p}{C_f}\right) \times 100\% \quad (2)$$

where C_p and C_f are the concentrations at the permeate and feed sides, respectively.

Stability

The GO-GN composite membranes were cut into rectangular pieces, and these were statically immersed in neutral solutions (pH = 6.8) at room temperature. After immersion for certain periods of time, the stabilities of the GO-GN composite membranes were recorded by taking pictures of the membrane.

3. Results and discussion

3.1 Characterization studies

The surface and cross-section of the GO-GN composite membranes with different proportions were characterized using SEM. As seen in Figs. 2 (A)-(E), GN was uniformly

distributed in the GO layer, and the resulting composite membranes were continuous without large holes or defects. These characteristics are key to the efficient separation process. With an increasing amount of GN, the GN morphology characteristics of the surface of the composite membranes gradually became prominent. As seen from Figs. 2 (a)-(e), the films' thickness gradually increased with an increase in GN content. A maximum of 420.4 nm was obtained with a GO-GN ratio of 0.5:0.1. According to Fig. 2 (F), there was almost a linear relationship between the thickness of the films and the amount of added GN, and this indicates that the thickness of the composite membranes can be precisely regulated by controlling the relative amount of GN.

To further analyze the microscopic structure of the GO-GN composite membranes, the microscopic morphologies of GO, GN, and GO_{0.5}-GN_{0.08} (mix of 0.5 mg of graphene oxide and 0.08 mg of single-layer graphene) were each characterized using TEM. Fig. 3 (A) shows GO that was prepared via the improved Hummers method. There are no impurities or obvious defects on the surface of pure GO, and this indicates that GO has excellent morphological characteristics. Fig. 3 (B) shows that the GN with obvious lamellar structure is transparent, and the size of the GN sheets is about 500-1000 nm. Fig. 3 (C) shows that GO and GN were successfully combined, and GN was attached to the GO layers.

Fig. 4 (a) shows the Raman spectral analysis of GO-GN composite membranes. Three peaks can be observed: the G peak (1580 cm⁻¹), D peak (1350 cm⁻¹), and 2D peak (2700 cm⁻¹). The G peak represents sp² carbon networks, and the D peak is generally used to explain the presence of disordered or amorphous carbon.

The ratio of the D peak strength (I_D) to G peak strength (I_G) (where I_D and I_G are the Raman intensities of the D

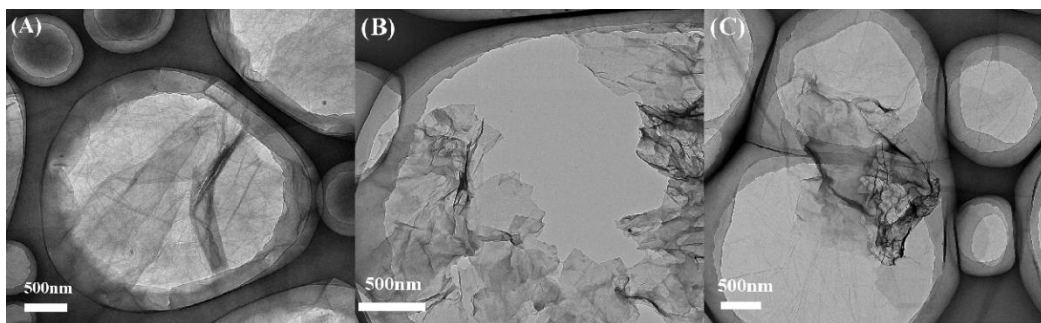


Fig. 3 (A) TEM images of GO. (B) TEM images of GN. (C) TEM images of $GO_{0.5}-GN_{0.08}$

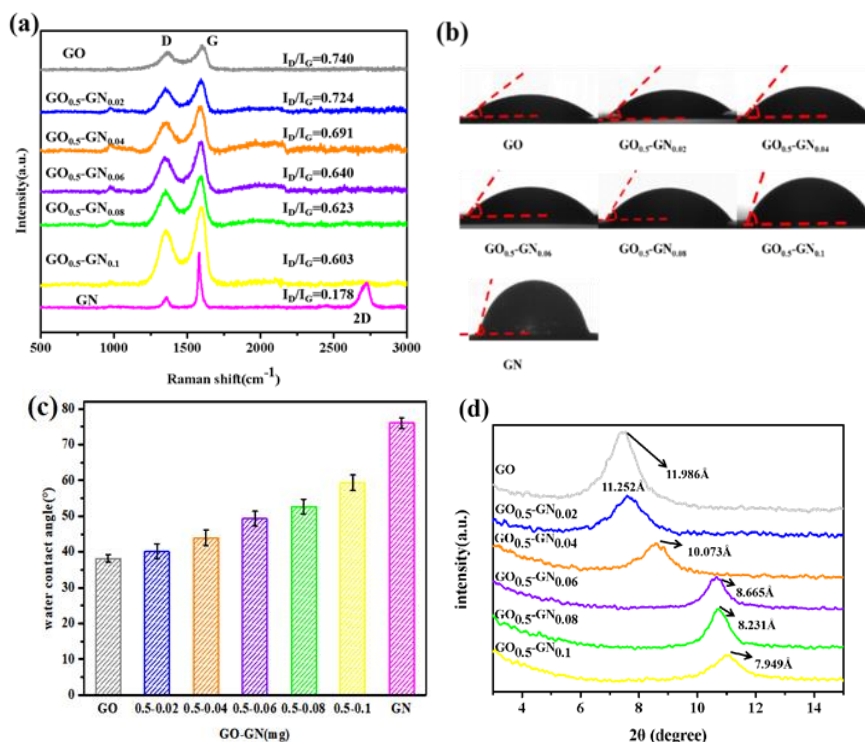


Fig. 4 (a) Raman spectroscopic analysis of the GO-GN composite membranes. (b) Photos of a water droplet on the surface of the GO-GN composite membranes. (c) Variations in water contact angle. (d) XRD analysis of the GO-GN composite membranes

band and G band, respectively) is widely used to evaluate graphite disorder (defects). It can also be used to distinguish GO from GN. When GO has more functional groups, a higher value of the I_D/I_G ratio (e.g., $I_D/I_G=0.74$) can be obtained. Raman spectra of all of the GO-GN composite membranes show intermediate behavior between GO and GN configurations (Fig. 4 (a)), indicating that GN was successfully interleaved between GO layers. That is, GN was dispersed in the whole GO matrix.

Water contact angle values of the GO-GN composite membranes were measured to study the hydrophilicity (Moradi *et al.* 2018). To detect differences in hydrophilicity of GO-GN composite membranes with different proportions of GO and GN, the water contact angle values were measured, and the results are shown in Figs. 4 (b)-(c). Because of the presence of hydrophilic oxygen-containing groups on GO sheets, the surface of the GO membrane is hydrophilic, and the contact angle of the GO membrane was

38.2° (Fig. 4 (c)). With an increase in GN content, the amount of GN on the surface of the GO-GN composite membranes increased. GN is hydrophobic, and thus, the overall hydrophilicity of the membrane was reduced. When the GN content was 0.1 mg, the water contact angle of the membrane was 59.32° (Fig. 4 (c)), and this indicates that the membranes were still hydrophilic in nature.

Changes in the layer spacing of the composite membranes were measured using XRD (Fig. 4 (d)). In a dry state, the d-spacing of the GO membrane was about 8.786 \AA (Fig. S2). In a wet state, the d-spacing of the GO membrane was about 11.986 \AA . The interlayer distance in the films in the wet state is larger than that in the dry state, and this is caused by interactions between the solvent and nanolayer in all of the membranes. With an increase in the GN content, the d-spacing of the membranes decreased. Compared to values reported in the relevant literature, it is determined that the d-spacing can be controlled to be smaller because

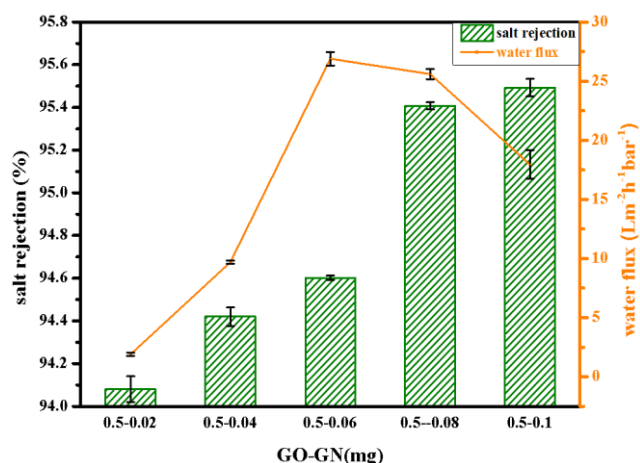


Fig. 5 Water flux and salt rejection of the GO-GN composite membranes with different proportions of GO and GN

Table 1 Comparison of the separation performance of the GO-GN membrane with other membranes reported in the literature

Membranes	Rejection	Ref.
GO- graphene	NaCl:88.3%	(Wei-Song <i>et al.</i> 2018)
RGO-OCNT	NaCl: 35.3%	(Zhang <i>et al.</i> 2018)
10%rPGM	NaCl: 5.3%	(Li <i>et al.</i> 2022)
RGO	RB:90%	(Fan <i>et al.</i> 2020)
GO/MXene	RB: > 99.5	(Liu <i>et al.</i> 2019)
150-GTM	RB:>97.2%	(Ye <i>et al.</i> 2023)
cGO/SAA	NaCl:80±2% RB:99±1%	(Chandio <i>et al.</i> 2020)
GO0.5-GN0.08	NaCl:95.4% RB:~100%	This work

we used single-layer GN that is very thin and can be mixed more evenly with GO. As seen Fig. 4(d), the layer spacing was reduced from about 11.986 Å to about 7.949 Å. These results confirm that the GO membranes that have added GN have adjustable spacing.

3.2 Nanofiltration performance

Water flux and salt filtration rate are two important parameters for testing the performance of nanofiltration films. Fig. 5 shows analysis of water flux and rejection for GO-GN composite membranes with different proportions of GO and GN. As seen in Fig. 5, rejection of inorganic salt by composite nanofiltration membranes gradually increased with an increase in the amount of GN, but the water flux first increased obviously and then decreased slightly. This is mainly because the introduction of the hydrophobic GN into GO improved the swelling of the composite membranes, decreased the d-spacing of the membranes (Fig. 4 (d)), and increased the thickness of the composite membranes (Fig. 2 (F)). The water flux of the membrane increased with an increase in GN content, as interactions (hydrogen bonding) between water molecules and oxygen functional groups in GO nanosheets were weakened by the insertion of GN. This

results in lower flow resistance and higher flux. For the pure GO membrane, when water passes through the oxidized region in the nanocapillary channels, hydrogen bonds form with the oxygen-containing functional groups, and this results in increased flow resistance. On the contrary, resistance in the nonoxidized region is very small. However, if there is too much GN, the thickness membranes increases, and this makes the path of water transport longer and reduces water flux. When the GN content was greater than 0.06 mg, water flux decreased (Fig. 5), and this is because the membrane was too thick. In this experiment, when the amount of GN was 0.08 mg, the rejection (95.4%) and water flux (26 L m⁻² h⁻¹ bar⁻¹) reached the optimal equilibrium point.

At the same time, we tested the rejection rate of RB (Rhodamine B) by the composite membranes. The highest adsorption peak of RB was 559 nm (Fig. S3), and the dye concentration was measured using a UV-vis spectrometer. The composite membranes show a good rejection performance for RB, as seen in Fig. S3(c). With an increase in GN content, the rejection of the composite membranes increased. This is also because the introduction of hydrophobic GN in GO improves the swelling of the composite membrane, reduces the d-spacing of the membrane, and increases the thickness of the composite membrane. Because the diameter of RB molecules is larger than that of NaCl molecules, when the GN content exceeded 0.6 mg, the rejection almost reached 100%. Compared with other membranes, the GO-GN membranes have high separation performance (as shown in Table 1).

The long-term stability of the membranes is very important for its separation performance. The stability of the GO-GN composite membranes was studied and compared to the stability of GO in aqueous solution. As seen in Fig. S4, the GO membrane disintegrated in aqueous solution after 4 days. In contrast, the GO-GN composite membranes were very stable; Specifically, they maintained their original structure even after 30 days. This is because the interlayer distance of GO and the repulsive hydration force between GO and water can be reduced by inserting GN into the GO. When the interlaminar spacing becomes compact, π - π lamellar attraction is enhanced, and this results in the high stability of the composite membranes.

4. Conclusions

In summary, a battery of novel GO-GN composite membranes were prepared for water treatment. The composite membranes were obtained by inserting GN into GO. The properties of the GO-GN composite membranes were evaluated using SEM, TEM, LAMAN, XRD, and contact angle tests. The results indicate that, the interlayer spacing of the membranes in a wet state decreased with an increase in the GN content. This is because that the GN that we used was single-layer and very thin, thus, it could be more evenly mixed with GO. Compared to recent studies, this method achieves a smaller layer spacing and more effective screening, and these characteristics further expand the application prospects of this method. In addition, incorporating GN into the GO layers can reduce the layer

spacing, increase the composite membrane thickness, and improve the rejection rate. Moreover, GN provides more low-friction nanocapillary channels, thus increasing the permeability of water. When the mass ratio of GO-GN in the membrane was 0.5-0.08, water flux was $26 \text{ L m}^{-2} \text{ h}^{-1} \text{ bar}^{-1}$, the NaCl rejection rate was about 95.4%, and the dye rejection rate was about 100%. Furthermore, the composite membranes showed high stability in aqueous solutions for a long time. Coupled with the membrane's excellent rejection and water flux, there are great opportunities for the application of these composite membranes in aqueous solutions.

Acknowledgments

This work was supported by the National Natural Science Foundation of China (Grant No.51005145 and 51075258), Shanghai Engineering Research Center of Marine Renewable Energy (Grant No.19DZ2254800), and the Instrumental Analysis Center and the Center for Advanced Electronic Materials and Devices of Shanghai Jiao Tong University.

References

- Abraham, J., Vasu, K.S., Williams, C.D., Gopinadhan, K., Su, Y., Cherian, C.T., Dix, J., Prestat, E., Haigh, S.J., Grigorieva, I.V., Carbone, P., Geim, A.K. and Nair, R.R. (2017), "Tunable sieving of ions using graphene oxide membranes", *Nature Nanotechnol.*, **12**, 546-550. <https://doi.org/10.1038/nnano.2017.21>.
- Buelke, C., Alshami, A., Casler, J., Lin, Y., Hickner, M. and Aljundi, I.H. (2019), "Evaluating graphene oxide and holey graphene oxide membrane performance for water purification", *J. Membr. Sci.*, **588**, 117195. <https://doi.org/10.1016/j.memsci.2019.117195>.
- Chandio, I., Janjhi, F.A., Memon, A.A., Memon, S., Ali, Z., Thebo, K.H., Pirzado, A.A.A., Hakro., A.A. and Khan, W.S. (2020), "Ultrafast ionic and molecular sieving through graphene oxide based composite membranes", *Desalination*, **500**, 114848. <https://doi.org/10.1016/j.desal.2020.114848>.
- Chen, L., Li, N., Wen, Z., Zhang, L., Chen, Q., Chen, L., Si, P., Feng, J., Li, Y., Lou, J and Ci, L. (2018), "Graphene oxide based membrane intercalated by nanoparticles for high performance nanofiltration application", *Chem. Eng. J.*, 12-18. <https://doi.org/10.1016/j.cej.2018.04.069>.
- Chen, X., Qiu, M., Ding, H., Fu, K. and Fan, Y. (2016), "A reduced graphene oxide nanofiltration membrane intercalated by well-dispersed carbon nanotubes for drinking water purification", *Nanoscale*, **8**, 696-705. <https://doi.org/10.1039/c5nr08697c>.
- Fan, X., Cai, C., Gao, J., Han, X. and Li, J. (2020), "Hydrothermal reduced graphene oxide membranes for dyes removing", *Sep. Purif. Technol.*, **241**, 116730. <https://doi.org/10.1016/j.seppur.2020.116730>.
- Haan, T.Y., Shah, M., Chun, H.K. and Mohammad, A.W. (2018), "A study on membrane technology for surface water treatment: Synthesis, characterization and performance test", *Membr. Water Treat.*, **9**(2), 69-77. <http://doi.org/10.12989/mwt.2018.9.2.069>
- Han, Y., Jiang, Y. and Gao, C. (2015), "High-flux graphene oxide nanofiltration membrane intercalated by carbon nanotubes", *ACS Appl. Mater. Interf.*, **7**, 8147. <https://doi.org/10.1021/acsami.5b00986>.
- Hirunpinyopas, W., Iamprasertkun, P., Bissett, M.A. and Dryfe, R.A. (2019), "Tunable charge/size selective ion sieving with ultrahigh water permeance through laminar graphene membranes", *Carbon*, **156**, 119-129. <https://doi.org/10.1016/j.carbon.2019.09.030>.
- Huang, H.H., Joshi, R.K., De Silva, K.K.H., Badam, R. and Yoshimura, M. (2019), "Fabrication of reduced graphene oxide membranes for water desalination", *J. Membr. Sci.*, **572**, 12-19. <https://doi.org/10.1016/j.memsci.2018.10.085>.
- Hung, W.S., Lin, T.J., Chiao, Y.H., Sengupta, A., Hsiao, Y.C., Wickramasinghe, S.R., Hu, C.C., Lee, K.R. and Lai, J.Y. (2018), "Graphene-induced tuning of the d-spacing of graphene oxide composite nanofiltration membranes for frictionless capillary action-induced enhancement of water permeability", *J. Mater. Chem. A*, **6**, 19445-19454. <https://doi.org/10.1039/C8TA08155G>.
- Jin, S., Gao, Q., Zeng, X., Zhang, R., Liu, K., Shao, X. and Jin, M. (2015), "Effects of reduction methods on the structure and thermal conductivity of free-standing reduced graphene oxide films", *Diamond Relat. Mater.*, 54-61. <https://doi.org/10.1016/j.diamond.2015.06.005>.
- Li, S., Lu, J., Zou, D., Cui, L., Chen, B., Wang, F., Qiu, J., Yu, T., Sun, Y. and Jing, W. (2022), "Constructing reduced porous graphene oxide for tailoring mass-transfer channels in ultrathin MXene (Ti₃C₂T_x) membranes for efficient dye/salt separation", *Chem. Eng. J.*, **457**, 141217. <https://doi.org/10.1016/j.cej.2022.141217>.
- Li, W., Wu, W. and Li, Z. (2018), "Controlling interlayer spacing of graphene oxide membranes by external pressure regulation", *ACS Nano*, **12**, 9309-9317. <https://doi.org/10.1021/acsnano.8b04187>.
- Liang, S., Wang, S., Chen, L. and Fang, H. (2020), "Controlling interlayer spacings of graphene oxide membranes with cationic for precise sieving of mono-/multi-valent ions", *Sep. Purif. Technol.*, **241**, 116738. <https://doi.org/10.1016/j.seppur.2020.116738>
- Liu, T., Liu, X., Graham, N., Yu, W. and Sun, K. (2019), "Two-dimensional MXene incorporated graphene oxide composite membrane with enhanced water purification performance", *J. Membr. Sci.*, **593**, 117431. <https://doi.org/10.1016/j.memsci.2019.117431>.
- Lyu, J., Wen, X., Kumar, U., You, Y., Chen, V. and Joshi, R.K. (2018), "Separation and purification using GO and r-GO membranes", *RSC Adv.*, **8**, 23130-23151. <https://doi.org/10.1039/C8RA03156H>.
- Moradi, R., Shariaty-Niassar, M., Pourkhalili, N., Mehrzadeh, M. and Niknafs, H. (2018), "PVDF/h-BN hybrid membranes and their application in desalination through AGMD", *Membr. Water Treat.*, **9**(4), 221-231. <http://doi.org/10.12989/mwt.2018.9.4.221>.
- Pachfule, P., Shinde, D., Majumder, M. and Xu, Q. (2016), "Fabrication of carbon nanorods and graphene nanoribbons from a metal-organic framework", *Nature Chem.*, **8**, 18-24. <https://doi.org/10.1038/nchem.2515>.
- Pei, S., Zhao, J., Du, J., Ren, W. and Cheng, H.M. (2010), "Direct reduction of graphene oxide films into highly conductive and flexible graphene films by hydrohalic acids", *Carbon*, **48**, 4466-4474. <https://doi.org/10.1016/j.carbon.2010.08.006>.
- Shao, F., Hu, N., Su, Y., Yao, L., Li, B., Zou, C., Li, G., Zhang, C., Li, H., Yang, Z. and Zhang, Y. (2020), "Non-woven fabric electrodes based on graphene-based fibers for areal-energy-dense flexible solid-state supercapacitors", *Chem. Eng. J.*, **392**, 123692. <https://doi.org/10.1016/j.cej.2019.123692>.
- Sun, Y., Yu, F., Li, C., Dai, X. and Ma, J. (2020), "Nano-/micro-confined water in graphene hydrogel as superadsorbents for water purification", *Nano Micro Lett.*, **12**, 1-14. <https://doi.org/10.1007/s40820-019-0336-3>.

- Sur, U. K., Saha, A., Datta, A., Ankamwar, B., Surti, F., Roy, S. D. and Roy, D. (2016), "Synthesis and characterization of stable aqueous dispersions of graphene", *Bull. Mater. Sci.*, **39**, 1-7. <https://doi.org/10.1007/s12034-015-0893-0>.
- Syama, S. and Mohanan, P.V. (2019), "Comprehensive application of graphene: Emphasis on biomedical concerns", *Nano Micro Lett.*, **11**, 97-127. <https://doi.org/10.1007/s40820-019-0237-5>.
- Tang, S., Jin, S., Zhang, R., Liu, Y., Wang, J., Hu, Z., Lu, W., Yang, S., Qiao, W., Ling, L. and Jin, M. (2019), "Effective reduction of graphene oxide via a hybrid microwave heating method by using mildly reduced graphene oxide as a susceptor", *Appl. Surf. Sci.*, **473**, 222-229. <https://doi.org/10.1016/j.apsusc.2018.12.096>.
- Thebo, K.H., Qian, X., Zhang, Q., Chen, L., Cheng, H.M. and Ren, W. (2018), "Highly stable graphene-oxide-based membranes with superior permeability", *Nature Commun.*, **9**, 1486. <https://doi.org/10.1038/s41467-018-03919-0>.
- Tiwari, S.K., Sahoo, S., Wang, N. and Huczko, A. (2020), "Graphene Research and their Outputs: Status and Prospect", *J. Sci. Adv. Mater. Devices*, **5**, 10-29. <https://doi.org/10.1016/j.jsamd.2020.01.006>.
- Toh, S.Y., Loh, K.S., Kamarudin, S.K. and Daud, W.R.W. (2014), "Graphene production via electrochemical reduction of graphene oxide: Synthesis and characterisation", *Chem. Eng. J.*, **251**, 422-434. <https://doi.org/10.1016/j.cej.2014.04.004>.
- Singh, V., Joung, D., Zhai, L., Das, S., Khondaker, S.I. and Seal, S. (2011), "Graphene based materials: Past, present and future", *Prog. Mater. Sci.*, **56**, 1178-1271. <https://doi.org/10.1016/j.pmatsci.2011.03.003>.
- Wan, Z., Wang, S., Haylock, B., Kaur, J., Tanner, P., Thiel, D., Sang, R., Cole, I.S., Li, X., Lobino, M. and Li, Q. (2019), "Tuning the sub-processes in laser reduction of graphene oxide by adjusting the power and scanning speed of laser", *Carbon*, **141**, 83-91. <https://doi.org/10.1016/j.carbon.2018.09.030>.
- Wang, Q., Zhao, G., Li, C. and Meng, H. (2019), "Orderly stacked ultrathin graphene oxide membranes on a macroporous tubular ceramic substrate", *J. Membr. Sci.*, **586**, 177-184. <https://doi.org/10.1016/j.memsci.2019.05.051>.
- Wang, X., Li, N., Zhao, Y. and Xia, S. (2018), "Preparation of graphene oxide incorporated polyamide thin-film composite membranes for PPCPs removal", *Membr. Water Treat.*, **9**(4), 211-220. <https://doi.org/10.12989/mwt.2018.9.4.211>.
- Wei, Y., Zhu, Y. and Jiang, Y. (2019), "Photocatalytic self-cleaning carbon nitride nanotube intercalated reduced graphene oxide membranes for enhanced water purification", *Chem. Eng. J.*, **356**, 915-925. <https://doi.org/10.1016/j.cej.2018.09.108>.
- Xi, Y.H., Hu, J.Q., Liu, Z., Xie, R., Ju, X.J., Wang, W. and Chu, L.Y. (2018), "Graphene oxide membranes with strong stability in aqueous solutions and controllable lamellar spacing", *ACS Appl. Mater. Interf.*, **8**, 15557-15566. <https://doi.org/10.1021/acsami.6b00928>.
- Xu, Q., Xu, H., Chen, J., Lv, Y., Dong, C. and Sreeprasad, T.S. (2015), "Graphene and graphene oxide: advanced membranes for gas separation and water purification", *Inorgan. Chem. Front.*, **46**, 417-424. <https://doi.org/10.1002/chin.201530322>.
- Ye, Z., Yang, L., Wang, Y., Jia, F., Li, Z., Yu, D., Mao, X., Huang, L. and Tang, J. (2023), "Graphene oxide membranes intercalated with titanium dioxide nanorods for fast infiltration and dye separation", *FlatChem*, **38**, 100488. <https://doi.org/10.1016/j.flatc.2023.100488>.
- You, Y., Sahajwalla, V., Yoshimura, M. and Joshi, R.K. (2016), "Graphene and graphene oxide for desalination", *Nanoscale*, **8**, 117-119. <https://doi.org/10.1039/C5NR06154G>.
- Yu, W. and Graham, N. (2017), "Development of a stable cation modified graphene oxide membrane for water treatment", *2D Mater.*, **4**, 045006. <https://doi.org/10.1088/2053-1583/aa814c>.
- Zhang, H., Quan, X., Chen, S., Fan, X., Wei, G. and Yu, H. (2018), "Combined effects of surface charge and pore size on co-enhanced permeability and ion selectivity through RGO-OCNT nanofiltration membranes", *Environ. Sci. Technol.*, **52**(8), 4827-4834. <https://doi.org/10.1021/acs.est.8b00515>.
- Zhang, N., Qi, W., Huang, L., Jiang, E., Bao, J., Zhang, X., An, B. and He, G. (2019), "Review on structural control and modification of graphene oxide-based membranes in water treatment: From separation performance to robust operation", *Chinese J. Chem. Eng.*, **27**, 1348-1360. <https://doi.org/10.1016/j.cjche.2019.01.001>.
- Zhang, Q., Qian, X., Thebo, K.H., Cheng, H.M. and Ren, W. (2018), "Controlling reduction degree of graphene oxide membranes for improved water permeance", *Sci. Bull.*, **63**, 788-794. <https://doi.org/10.1016/j.scib.2018.05.015>.
- Zhang, Y. and Chung, T.S. (2017), "Graphene oxide membranes for nanofiltration", *Curr. Op. Chem. Eng.*, **16**, 9-15. <https://doi.org/10.1016/j.coche.2017.03.002>.
- Zhao, G., Hu, R., Zhao, X., He, Y. and Zhu, H. (2019), "High flux nanofiltration membranes prepared with a graphene oxide homo-structure", *J. Membr. Sci.*, **585**, 29-37. <https://doi.org/10.1016/j.memsci.2019.05.028>.
- Zheng, S., Tu, Q., Urban, J.J., Li, S. and Mi, B. (2017), "Swelling of graphene oxide membranes in aqueous solution: Characterization of interlayer spacing and insight into water transport mechanisms", *Acs Nano*, **11**, 6440-6450. <https://doi.org/10.1021/acsnano.7b02999>.

CC

Appendix

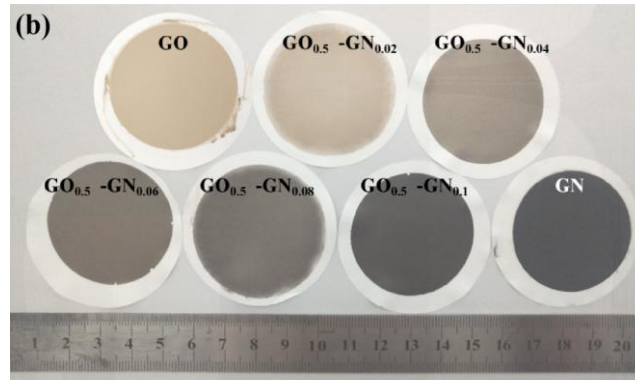


Fig. S1 Photographs of the GO-GN composite membranes with different relative compositions

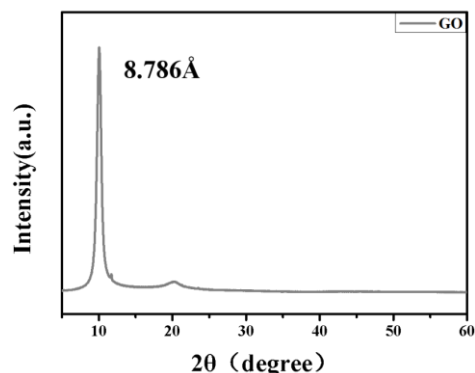


Fig. S2 XRD analysis of the GO membrane in dry state

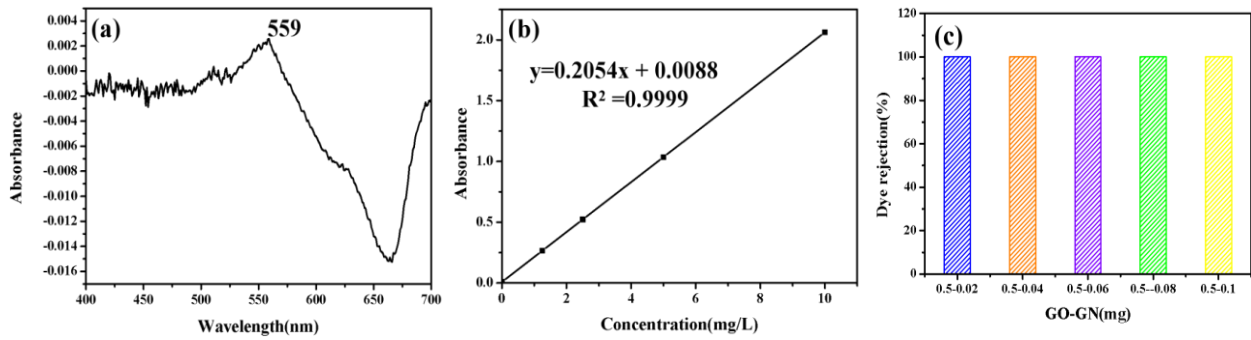


Fig. S3 (a) Ultraviolet absorption spectrum of RB (b) Standard curve for RB concentration and absorbance (c) RB rejection of GO-GN composite membranes with different proportion

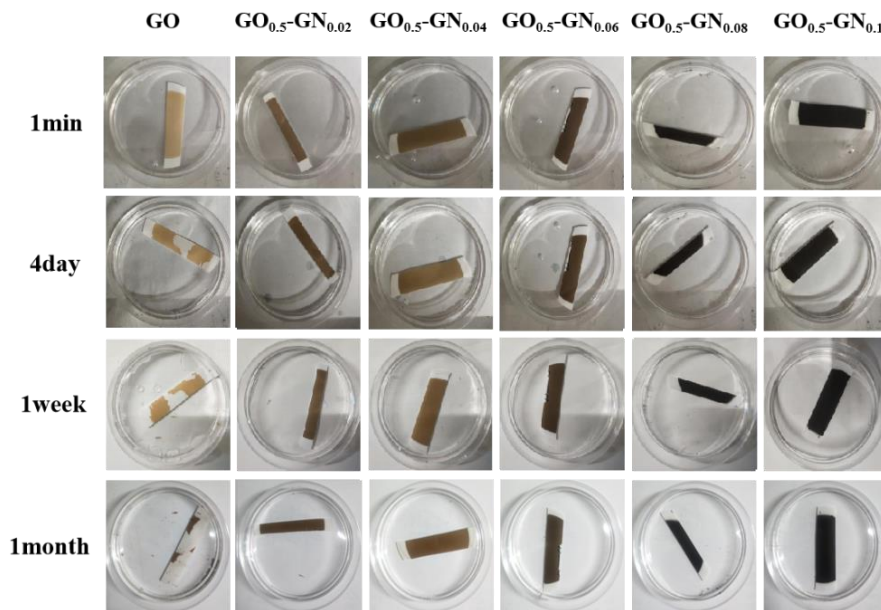


Fig. S4 Stability of GO-GN composite membranes with different proportion in water at pH=6.8